

EVALUATION OF EARTHQUAKE-INDUCED SLIDING
IN ROCKFILL DAMS

HIROYUKI WATANABE*, SEISHIRŌ SATŌ** and KYŌKO MURAKAMI**

ABSTRACT

The relation between the factor of safety obtained from dynamic response analyses on arbitrary potential sliding surface of a rockfill dam and the one obtained from conventional method such as slice method has been made clear by introducing a concept of equivalent instantaneous seismic coefficient.

Throughout many numerical experiments of dynamic response analyses conducted on a typical rockfill dam section with sinusoidal ground motions of various kinds of accelerations and periods, a simple expression for the sliding permanent displacements has been obtained as a function of maximum equivalent instantaneous seismic coefficient and duration of sliding which is independent of the scale and location of sliding surface, the period of ground motion and the amplitude of ground acceleration. This formula has been applied to the simplified evaluation for the sliding permanent displacements in the cases with the ground motions of recorded accelerograms.

Acceleration response spectra of many recorded accelerograms have been calculated and the ratio of each maximum value to peak ground acceleration has been plotted against corresponding predominant period. With this diagram the amplitude of equivalent sinusoidal ground acceleration has been specified as 0.5 to 0.6 of peak ground acceleration in conservative side.

Combining above formula with the magnification factors of the equivalent instantaneous seismic coefficients in the potential sliding circles near crest, an expression for the relationship between the amplitude of above equivalent sinusoidal ground acceleration and the earthquake-induced sliding displacement at near crest has been derived. Giving certain amount of allowable permanent displacement, an earthquake-resistant design diagram for rockfill dams concerning with the equivalent sinusoidal ground acceleration has been proposed.

Key words : dam, (dynamic response analysis), earthquake, rockfill, safety factor, (seismic coefficient) (IGC : E 8/H 4)

INTRODUCTION

Because of the recent advancement of

technique in numerical analyses with the spread of electronic computer, dynamic response analyses are commonly applied to

* Saitama University, Urawa, Saitama.

** Kaihatsu Keisan Sentā Co., Ltd., Tokyo.

Manuscript was received for review on September 19, 1983.

Written discussions on this paper should be submitted before April 1, 1985, to the Japanese Society of Soil Mechanics and Foundation Engineering, Sugayama Bldg. 4 F, Kanda Awaji-cho 2-23, Chiyoda-ku, Tokyo 101, Japan. Upon request the closing date may be extended one month.

the structural or stress analyses in the seismic designs of soil structures such as slopes, embankments, fill dams, etc. Nevertheless, it can not be said that we have reliable basis for evaluating the stability of these structures with computed results except for the cases of liquefaction. Among earlier studies on the assesment of seismic stability of fill dams one of the authors proposed a procedure to evaluate the seismic stability based on the distribution of the lowest computed point factors of safety over the cross section (Watanabe, 1973). Another procedure on the basis of accumulated strain induced by earthquake motions was proposed and applied to the seismic design of Los Angeles dam constructed in the place of the Lower San Fernando dam in which upstream shell a major slide occurred as a result of the 1971 San Fernando Earthquake (Seed et al, 1973). This procedure was developed on the basis of the liquefaction assessment method using dynamic response analyses and has been developed into the method for earthquake-resistant design of earth dams based on the evaluation of the deformations due to earthquake motions (Seed, 1979). The concept of this procedure is recently applied to the static finite element analyses where the seismic induced settlements and deformations in soil structures are estimated with the static secant modulus of the materials taking into account of the decrease of it due to cyclic loading (Nakamura et al, 1982; Sasaki et al, 1982).

On the other hand the relation between the factor of safety obtained from so-called pseudo-static method and the one evaluated from the dynamic response analyses was not clarified until a recent date. Attempts by one of the authors to interpret above relation have partially proved successful by introducing the concept of equivalent instantaneous seismic coefficient (Watanabe et al, 1981). Combining this seismic coefficient with the basic elements of a procedure for evaluating the potential deformations of an embankment dam due to earthquake motion proposed first by Professor N. M. Newmark (Newmark,

1965) and developed by Professor H. B. Seed (Seed, 1979), an expression for earthquake-induced horizontal permanent displacement of the potential sliding mass of a rockfill dam has been derived from yield acceleration defined as being equivalent to the resisting resultant force on the sliding surface and surplus active acceleration (Watanabe et al, 1981).

In this study the results of dynamic response analyses conducted on an actual rockfill dam with a design earthquake motion have been shown to provide convincing evidence of the validity in above mentioned relation between the factors of safety by two methods. A simple formula has been derived for the horizontal permanent displacements of the potential sliding masses of a rockfill dam as a function of maximum equivalent instantaneous seismic coefficient and duration of sliding throughout many numerical experiments of dynamic response analyses conducted on a typical rockfill dam section with sinusoidal ground motions of various kinds of accelerations and periods.

This formula derived in this study has been applied to predict the critical ground acceleration for earthquake resistant design of a rockfill dam on the basis of the amount of earthquake-induced sliding permanent displacement at near crest.

EQUIVALENT INSTANTANEOUS SEISMIC COEFFICIENT AND FACTOR OF SAFETY

The point factors of safety of all elements inside the rockfill dam body will be computed with the response stresses obtained from a dynamic response analysis at every time increment. When there is a large number of elements of which point safety factors are unity or under, a rectangular particle cut out by the planes perpendicular to the principal stresses is examined in each element. When the compressive stress acting on this rectangular particle increases and becomes greater than the allowable stress defined by Mohr-Coulomb Criteria, we may

consider that local sliding takes place in the directions forming the angles of $(\pi/4 \pm \phi)$ from acting plane, where ϕ is the angle of internal friction. The plane along each direction is called "mobilized plane" and is in two directions. In the case when the directions of mobilized planes being connected in succession are extending outside the dam body we regard this state as what will lead to macroscopic sliding failure. This successive plane forms a potential sliding surface.

The contour of every potential sliding surface becomes to be nearly perfect circle as shown in Fig. 1. Total 17 potential sliding circles were thus defined in the previous paper throughout many numerical experiments. All representative potential sliding circles for a rockfill dam concentrated upon the surface layer of the dam body. So that it may be said that composite sliding surfaces of a rockfill dam consist of several small and shallow sliding circles (Watanabe and Baba, 1981).

With the response accelerations at every moment acting on a sliding mass bounded by a potential sliding circle, "equivalent instantaneous seismic coefficient (k_e)" was defined in the previous paper (Watanabe and Baba, 1981) as follows

$$k_e = \frac{\iint_c \rho(x, y) \cdot \alpha(x, y) dx dy}{g \cdot \iint_c \rho(x, y) dx dy} \quad (1)$$

where $\alpha(x, y)$ is the response acceleration on any point (x, y) in the sliding mass, $\rho(x, y)$ is the density at the point and g is acceleration of gravity. Eq. (1) times g is a ratio of the integrated inertia force over

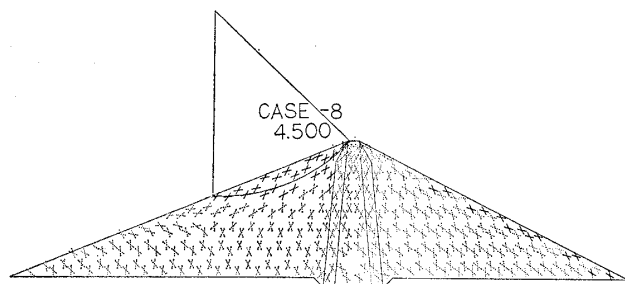


Fig. 1. Distribution of mobilized plane (Example 1)

the sliding mass to its total weight and represents an average response acceleration over the mass at every moment. Therefore the product of above seismic coefficient by the weight of the mass is equivalent to the total inertia force acting on the mass at every moment.

The yielding acceleration corresponding to the resisting force along a potential sliding surface against earthquake motion was derived in the previous paper (Watanabe and Baba, 1981) by equating driving moment, which is determined from the equivalent instantaneous seismic coefficient multiplied by the weight of the sliding mass, to the resisting moment and is written in the following form of seismic coefficient

$$k_R = F_S \cdot k_e + (F_S - 1) \tan \beta^* \quad (2)$$

where k_R is "yielding seismic coefficient", β^* is the angle between the radius of the sliding circle passing through the center of gravity of the sliding mass and the vertical, and F_S is the dynamic factor of safety written as follows

$$F_S = \frac{\sum \tau_{Ri} \cdot l_i}{\sum \tau_i \cdot l_i} \quad (3)$$

The suffix "i" in above equation represents the number of finite element through which the sliding line passes and l_i represents the length of the line cut out by the element.

The time history of F_S has been very similar to the one of k_e in all dynamic response analyses of soil structures which the authors have conducted so far. The times when the peaks and bottoms appear in the time history of F_S agree correctly with those of k_e . For examples, with the results of a dynamic response analysis conducted on a rockfill dam at "O" site in middle Japan which is 98 meter in height and has a design cross section as shown in Fig. 2(b), the value of k_e at every time when the peak or bottom appears in above time history has been plotted against the corresponding value of F_S and Fig. 2(a) has been obtained. The input earthquake motion is the accelerograms of TR component of Kaihoku Bridge in the 1978 Miyagiken-Oki Earthquake and is shown in Fig. 2(c).

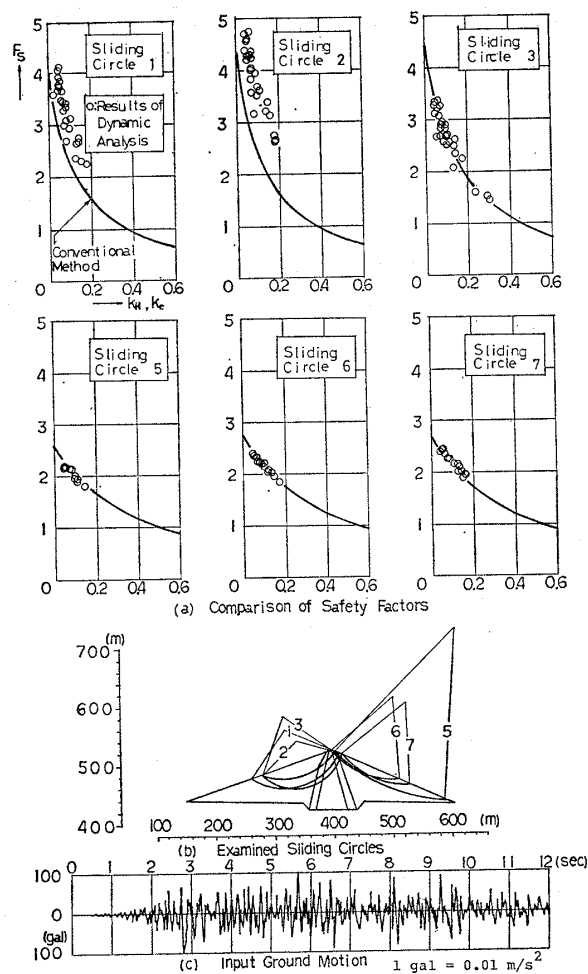


Fig. 2. Comparison of the factors of safety by two methods

Total 6 potential sliding circles have been examined as shown in Fig.2(b). Almost all of them have been determined by above method except for some circles decided by current design method. The solid lines in Fig.2(a) represent the relationship between horizontal seismic coefficient " k_H " and F_s obtained from the conventional method, that is, slice method in this paper.

The comparison of the relationships both between k_H and F_s and between k_e and F_s obtained from conventional method and dynamic response analysis method respectively indicates that both relationships agree well as shown in Fig.2(a) though the values of F_s are slightly larger in the latter. As we have seen it may be concluded that the relationship between F_s and k_e at every moment obtained from dynamic response

analysis is same one as obtained from conventional method, that is, the factor of safety with respect to sliding is to be nearly equal if only the load or the seismic coefficient applied to the sliding mass is same, though the method of analysis is different.

PERMANENT DISPLACEMENT OF THE MASS ON POTENTIAL SLIDING SURFACE DUE TO EARTHQUAKE MOTION

The behavior of the mass on an arbitrary potential sliding surface being taken into account, the resultant force along the surface is in a state of equilibrium with the inertia force of the mass until the mass begins to slide, however, in the state where the value of the resultant equivalent instantaneous seismic coefficient containing vertical component is greater than k_R sliding will take place. As soon as sliding takes place the surplus acceleration in excess of this yielding seismic coefficient does not be transmitted from the dam body to the sliding mass, however, the relative acceleration on the mass to the dam body becomes larger to the extent of this surplus acceleration in the coordinates fixed on the dam body below the mass, so that the mass moves with this surplus acceleration. The acceleration of the dam body below the sliding mass decreases and becomes less than the yielding acceleration in the subsequent state, then the sign of the relative acceleration is revised and the brakes will be put on the sliding mass.

All cases of the numerical experiments in this paper are summarized in Table 1. E(300) and E(200) in the table represent the cases of dynamic response analyses with the ground motions of the accelerograms of E1 Centro 1940 NS with peak acceleration of 300 gal (3.0 m/s²) and 200 gal (2.0 m/s²) respectively. H(450) and H(300) represent the cases with the accelerogram of Hiuganada 1968 with peak acceleration of 450 gal (4.5 m/s²) and 300 gal (3.0 m/s²) respectively. The acceleration spectra of the Hiuganada accelerogram are shown in Fig.3. The

Table 1. Analyzed cases

(a) Sinusoidal Cases					
A_0 (gal)	150	200	300	450	600
T (sec)					
0.125		Case B	Case 4	Case 2	Case 1
0.250		Case A	Case 6	Case 3	
0.375		Case 8	Case 7	Case 5	
0.500	Case C	Case 8	Case 7		
0.625	Case 10	Case 9			

1 gal = 0.01 m/s²

(b) Observed Ground Motion Cases			
Peak Acc.	200	300	450
Earthquake			
E 1 CENTRO 1940NS	Case E(200)	Case E(300)	
HIUGANADA 1968		Case H(300)	Case H(450)

response characteristics of tested rockfill dam section were discussed for the cases No.1 to No.8 and the case No. A in the previous paper (Baba and Watanabe, 1979). The cases No.9, No.10, No.B, No.C, No.E (200) and No.H(450) are newly added in this paper. The dynamic values of materials, the results of initial stress analyses and the cross section

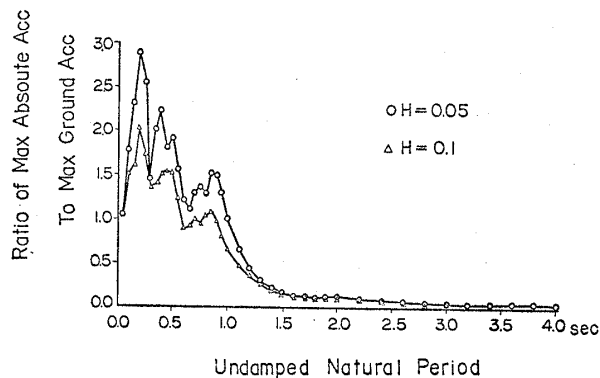


Fig. 3. Response spectra of input earthquake motion (Hiuganada 1968)

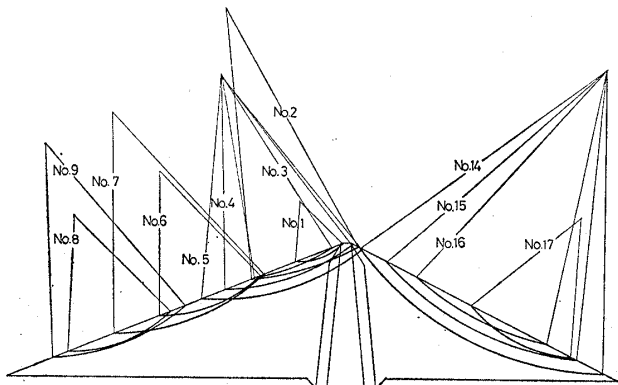


Fig. 4. Representative potential sliding circles

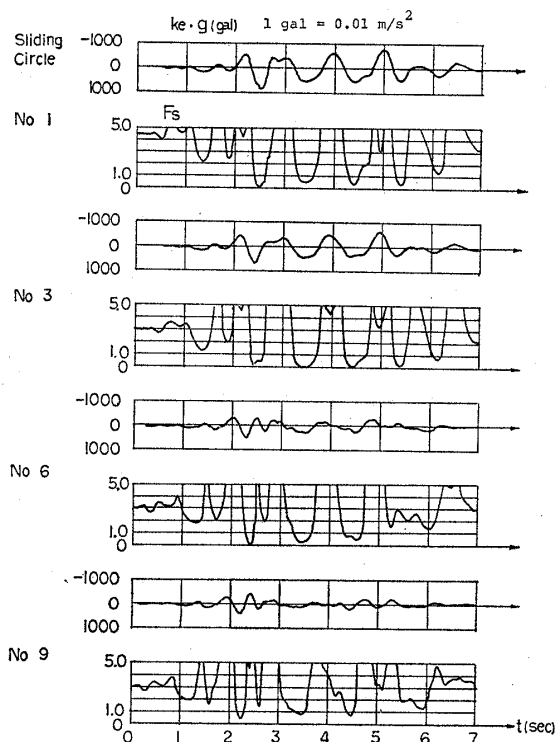


Fig. 5. Time histories of equivalent instantaneous seismic coefficient and factor of safety (E(300))

(the height of 153 m; the slopes of 1 : 2.6 in the up stream and 1 : 2.0 in the down stream sides respectively) are same as those used in above paper.

Among the 17 representative potential sliding circles defined in the previous paper only 12 circles have shown so significant amount of permanent displacement throughout the numerical experiments in this paper that we can consider sliding will take place. They are the circles of No.1 to No.9 and No.15 to No.17 as shown in Fig.4. Several examples concerning the time histories of the equivalent instantaneous seismic coefficient and the factor of safety for some of above potential sliding circles are shown in Fig.5. As stated before it may be said that the shapes of both time histories are very similar to each other.

In the previous paper (Watanabe and Baba, 1981) the horizontal permanent displacement " D_R " of a sliding mass due to the surplus acceleration $(k_e - k_R)g$ was defined as follows

$$D_R = \int_{t_0}^{t_1} \int_{t_0}^{\tau} (k_e - k_R) \cdot g d\tau dt \quad (4)$$

where t_0 is the time when F_s becomes equal to 1 in the beginning, t_1 is the time when the velocity of the sliding mass becomes zero. Fig. 6 shows an example of horizontal permanent displacement due to earthquake motion, that is, of progressive failure of slope thus calculated for the sliding circle No. 3 shown in Fig. 4.

In the usual dynamic response analyses of soil structures including those in this paper an equivalent linear FEM procedure is used where the non-linear stress-strain hysteresis curves are linearized into the secant moduli and the equivalent linear damping constants which vary with the amplitude of strain. Therefore, the calculation is being continued on the elastic continuum of complete structure without separating the sliding mass though the

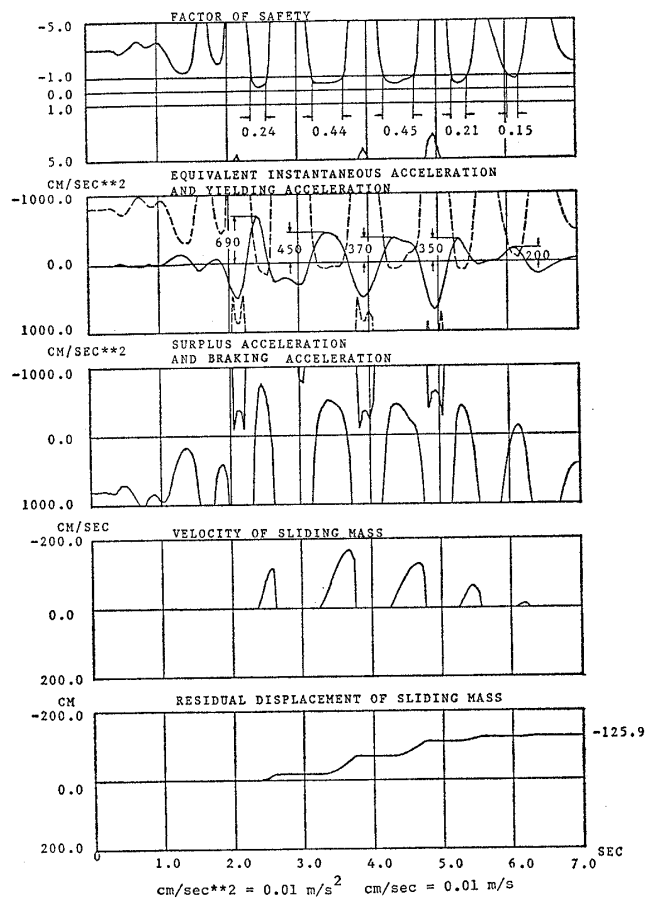


Fig. 6. Progressive failure of slope of rockfill dam (Circle No. 3)

Table 2. Residual horizontal displacement (D_R), duration (t_d) and instantaneous equivalent seismic coefficient ($k_{em} \cdot g$) obtained from numerical experiment

Sliding Circle No.	Ground Motion		Numerical Result		
	T (sec)	A_0 (gal)	t_d (sec)	D_R (cm)	$k_{em} \cdot g$ (gal)
1	0.375	200	0.0355	0.032	382
	0.375	300	0.0724	0.492	457
	0.375	450	0.0806	0.834	502
	0.500	200	0.0942	0.784	453
	0.500	300	0.1302	3.561	609
	0.625	150	0.0975	0.639	418
2	0.625	200	0.1746	6.447	569
	0.375	450	0.0180	0.003	198
	0.500	200	0.0929	0.527	323
	0.500	300	0.1230	2.060	372
	0.625	150	0.0734	0.155	286
	0.625	200	0.1625	4.822	449
3	0.375	200	0.0811	0.567	229
	0.375	300	0.0946	0.951	255
	0.375	450	0.1002	1.126	254
	0.500	150	0.1208	1.984	293
	0.500	200	0.1551	4.693	398
	0.500	300	0.1698	7.099	435
4	0.625	150	0.1732	5.229	320
	0.625	200	0.2184	12.190	402
	0.500	200	0.1004	0.850	301
	0.500	300	0.1117	1.713	323
	0.625	150	0.0308	0.007	249
	0.625	200	0.1408	2.715	347
5	0.625	200	0.0576	0.048	291
6	0.250	300	0.0237	0.007	331
	0.250	450	0.0552	0.293	418
	0.375	300	0.0931	1.036	458
	0.375	450	0.1180	2.683	597
	0.500	200	0.0751	0.367	317
	0.500	300	0.1153	1.821	484
7	0.625	150	0.1294	1.825	300
	0.625	200	0.1046	0.934	279
	0.375	300	0.0843	0.665	384
	0.375	450	0.1060	1.890	497
	0.500	300	0.1167	1.555	477
	8	0.250	300	0.0117	0.001
0.250		450	0.0491	0.156	351
0.375		300	0.0829	0.910	406
0.375		450	0.1107	2.775	582
0.500		200	0.1014	0.913	382
0.500		300	0.1432	4.949	494
9	0.625	150	0.0486	0.040	272
	0.250	450	0.0190	0.002	318
	0.375	300	0.0829	0.873	393
	0.375	450	0.1090	2.901	561
	0.500	200	0.1043	1.025	375
	0.500	300	0.1457	5.102	484
14	0.625	150	0.0745	0.162	268
	0.625	200	0.0274	0.005	225
	0.250	450	0.0559	0.348	608
	0.375	450	0.0805	0.669	668
	0.375	450	0.0597	0.169	525
	17	0.250	450	0.0460	0.166
0.375		450	0.1007	2.127	792

1 gal = 0.01 m/s²

equivalent instantaneous seismic coefficient exceeds the yielding one. In elastic continuum the absolute value of surplus acceleration on a sliding surface is equal to the one of the sliding mass because of the equilibrium, and $(k_e - k_R)g$ is approximately

adopted as the surplus acceleration. The word "approximately" is used advisedly here because the response of dam body is to be different according to whether the sliding mass is separated or not. However in rock-fill dams, as stated before, all the potential sliding circles are small and shallow so that the weight of sliding mass is considerably small comparing to the total weight of dam body. And so, it may be considered that the response acceleration on the sliding surface is not affected significantly by whether the sliding mass is separated or not and that above procedure will be valid as a first order approximation. We are now examining the dynamic response analysis method where sliding elements are introduced and have a plan to clarify the extent of error in this paper.

CHARACTERISTICS OF THE PERMANENT SLIDING DISPLACEMENT PER ONE PERIOD IN THE STEADY STATE RESPONSE OF A DAM DUE TO SINUSOIDAL GROUND MOTIONS

In each of 13 cases in Table 1(a) the horizontal sliding permanent displacement per one period due to sinusoidal ground motion (D_R ; cm) has been calculated for each of all 12 potential sliding circles shown in Fig.4 and the results are summarized in Table 2. The characteristics of D_R has been examined in every one of various sorts of parameters such as the period of ground motion (T (s)), the amplitude of ground acceleration A_0 (gal, $\times 0.01 \text{ m/s}^2$), duration of sliding t_d (s) and the amplitude of the equivalent instantaneous seismic coefficient k_{em} .

As a final result Fig.7 has been obtained and a simple regression curve has been drawn. As a upper envelope for the regression curve following simple formula has been derived.

$$D_R = \frac{1}{2} (k_{em} \cdot g) \cdot t_d^2 \quad (5)$$

As observed from Fig.7 this formula is obviously independent of the scale and

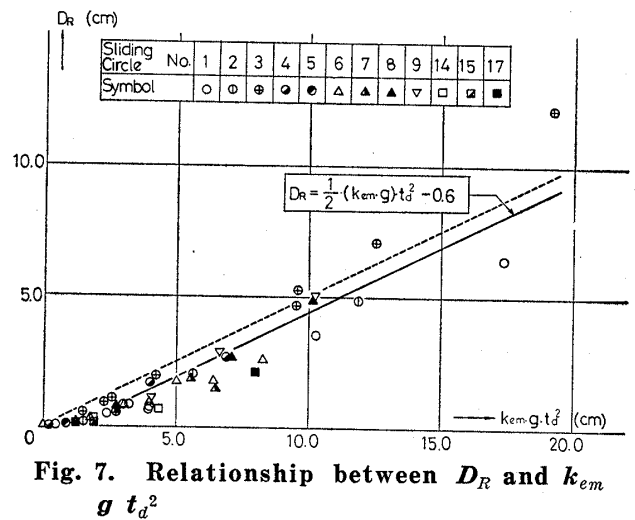


Fig. 7. Relationship between D_R and $k_{em} g t_d^2$

location of sliding surface, the period of ground motion and the amplitude of ground acceleration.

One of the physical meanings of the formula will be that the sliding mass under the constant acceleration of $k_{em}g$ starts to move with zero initial velocity and reaches at the place D_R (cm) distant from the initial position. Transforming Eq. (5) after multiplying both sides by the mass "m" following expression is obtained

$$m \cdot \left(\frac{D_R}{t_d} \right) = \frac{1}{2} (m \cdot k_{em} \cdot g) \cdot t_d \quad (6)$$

and the physical meaning of above equation will be that the impulse of the inertia force of the sliding mass during t_d owing to the acceleration $k_{em}g$ is equal to two times of the momentum of the mass moving with average velocity of D_R/t_d .

The availability of Eq. (5) makes it easy to estimate approximately the permanent displacement due to observed or artificial earthquake motion. Letting the duration of F_s under unity and the peak value of the equivalent instantaneous seismic coefficient be t_d and k_{em} respectively in Eq. (5) and adding together all of D_R thus calculated over total duration of the earthquake motion, the accumulated permanent displacement will be estimated as follows

$$D_f = \sum \frac{1}{2} (k_{em} \cdot g) \cdot t_d^2 \quad (7)$$

The number of summing up in Eq. (7) is

to be the one of the occurrence of the situation where F_s becomes under unity for total duration of the earthquake motion. In Fig. 6, by way of an example, each figure of both above mentioned durations and peak values of equivalent instantaneous seismic coefficient is written. Examples as to the results of above approximate estimation for the permanent displacement due to earthquake motion are summarized for the case of E(300) in Table 3. The results calculated exactly from Eq. (5) are shown together in the table. The coincidence of both results is considerably well.

AMPLITUDE OF EQUIVALENT INSTANTANEOUS SEISMIC COEFFICIENT CORRESPONDING TO CERTAIN AMOUNT OF PERMANENT DISPLACEMENT DUE TO EARTHQUAKE GROUND MOTION

Plotting the horizontal sliding permanent displacement per a period of sinusoidal ground motion (D_R) and the duration of F_s under unity (t_d) in logarithmic scale respectively Fig.8 has been obtained. The regression curve is expressed as follows

$$t_d = 1.67 \cdot \left(\frac{D_R}{H} \right)^{0.29} \quad (8)$$

Above relationship is independent of the scale and location of sliding circle, the period of ground motion and the amplitude of ground acceleration similar to Eq. (5).

Denoting the sliding permanent displacements and the durations of F_s under unity

Table 3. Residual displacement calculated from proposed method (case : E 300)

Sliding Circle No.	Proposed Method D_R^* (cm)	Numerical Results D_R (cm)	Error (%) $\frac{D_R^* - D_R}{D_R}$
1	33.643	21.664	-55.3
2	54.062	41.611	29.9
3	110.860	125.587	-11.7
4	54.667	44.530	22.8
5	21.447	14.909	44.1
6	23.954	28.088	-14.7
7	15.431	14.324	7.7
8	4.054	3.262	24.2
9	5.662	3.566	58.8

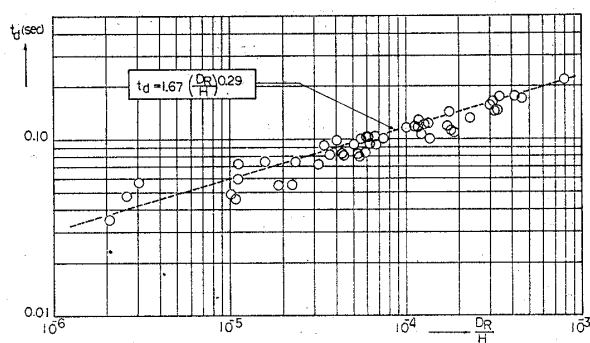


Fig. 8. Relationship between duration of $F_s < 1$ (t_d) and permanent displacement (D_R) against sinusoidal ground motion

generated by the ground motions of observed accelerograms as shown in Table 1(b) by D_f and t_f respectively, and plotting all of them calculated for all potential sliding circles as shown in Fig.4 in logarithmic scale too, Fig.9 has been obtained. The regression curve is expressed as follows

$$t_f = 10.7 \left(\frac{D_f}{H} \right)^{0.435} \quad (9)$$

Above relationship is also independent of the scale and location of sliding circle, the peak ground acceleration and even the sorts of accelerograms in the extent of those shown in Table 1(b).

Assuming that any ground accelerogram is replaced by "N" waves of the equivalent sinusoidal ground motion so as to generate same amount of sliding permanent displacement as D_f and letting the duration of F_s under unity per a period of this equivalent sinusoidal ground acceleration be expressed

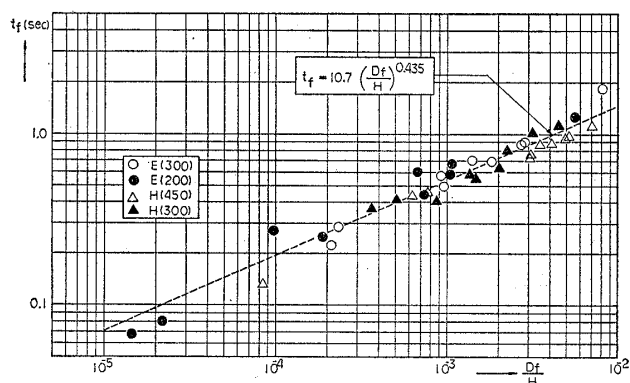


Fig. 9. Relationship between duration of $F_s < 1$ (t_f) and permanent displacement (D_f) against earthquake ground motion

by t_d , then t_f in Eq. (9) becomes

$$t_f = N \cdot t_d \quad (10)$$

Eliminating t_d and D_R from Eqs. (5), (8), (9) and (10) a relationship between the sliding permanent displacement due to ground earthquake motion (D_f), the number of equivalent sinusoidal ground waves (N) and the amplitude of the equivalent instantaneous seismic coefficient on arbitrary sliding circle (k_{em}) due to the equivalent sinusoidal ground motion has been derived as follows

$$k_{em} \cdot g = 373 \cdot (D_f)^{0.63} \cdot N^{-1.45}$$

where $H=153$ (m) has been substituted in Eq. (9). Rounding up the exponents of D_f and N in conservative side, following expression has been obtained.

$$k_{em} \cdot g = 373 \cdot (D_f)^{3/5} \cdot N^{-3/2}$$

Expressing the term of D_f in non-dimensional one above equation can be expressed as follows

$$k_{em} \cdot g = 123 \cdot g \cdot \left(\frac{D_f}{H} \right)^{3/5} \cdot N^{-3/2} \quad (11)$$

With above equation we have obtained a diagram concerning k_{em} and D_f as shown in Fig. 10.

ALLOWABLE EQUIVALENT SINUSOIDAL GROUND ACCELERATION CORRESPONDING TO GIVEN CRITICAL DEFORMATION AT CREST

Consideration on the Effect of Non-Linear Dynamic Constants

The dynamic values of materials used in calculations of the numerical experiments in this paper have the characteristics of parabolic

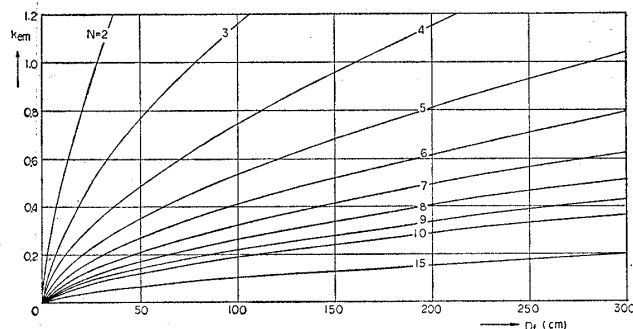


Fig. 10. Relationship between k_{em} and D_f

strain amplitude dependency and are written by the following equations

$$\frac{G}{G_0} = \frac{1}{1 + \gamma/\gamma_r} \text{ and } h = h_1 \cdot \frac{\gamma/\gamma_r}{1 + \gamma/\gamma_r} + h_2 \quad (12)$$

Eliminating the term of strain from above equations following expression can be derived

$$h = h_1 \cdot \left(1 - \frac{G}{G_0} \right) + h_2 \quad (13)$$

where G_0 is dynamic shearing modulus of micro-strain amplitude, h_1 is maximum value of the damping constant measured in the dynamic tri-axial compression test and h_2 is the damping constant due to dissipation of vibrating energy to ground assumed from earthquake observations and vibration tests on prototype dams.

The fundamental period of fill dams in the plane strain condition was derived by Matsumura (Matsumura, 1934) and is expressed by the following equation

$$T_1 = \alpha^* \cdot \sqrt{\rho/G} \cdot H \quad (14)$$

Expressing the fundamental period for micro-strain amplitude by $T_{1.0}$ following equation is derived from Eq. (14).

$$\frac{G}{G_0} = \left(\frac{T_{1.0}}{T_1} \right)^2 \quad (15)$$

Denoting the deviation of the fundamental period due to non-linear material properties by " τ " as follows

$$\frac{T_1 - T_{1.0}}{T_{1.0}} = \tau \text{ or } T_1 = T_{1.0} \cdot (1 + \tau) \quad (16)$$

and substituting it into Eq. (13) with Eq. (15) following equation can be derived

$$h = h_1 \cdot \left\{ 1 - \frac{1}{(1 + \tau)^2} \right\} + h_2 \quad (17)$$

Limiting the discussion within the response characteristics of dam body near the crest, the magnification factor of response acceleration in resonance is approximately expressed by h in following form.

$$M = \frac{A_c}{A_0} = \frac{1}{2h} \quad (18)$$

The magnification factor decreases as the amplitude of ground acceleration increases as shown in Fig. 11 which has been obtained from the numerical experiments in this paper

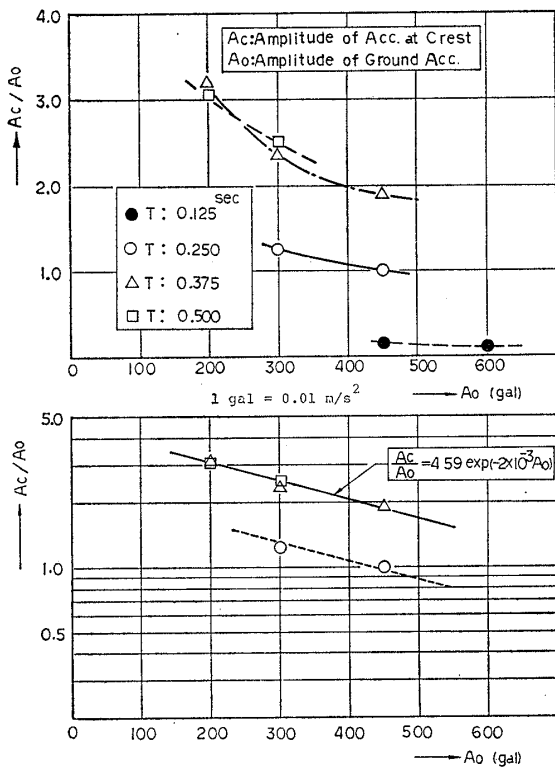


Fig. 11. Amplification factor of response acceleration at crest

and is very similar to the one obtained in dynamic model tests conducted before (Watanabe, 1977). The regression curve for the relationship between M and A_0 can be written in the following form.

$$M = M_0 \cdot \exp(-\beta \cdot A_0) \quad (19)$$

Substituting Eq. (18) with Eq. (19) for Eq. (17), following equation concerning the deviation of the fundamental period due to material non-linearity has been derived.

$$\tau = \sqrt{\frac{2h_1 \cdot M_0 \cdot \exp(-\beta \cdot A_0)}{2(h_1 + h_2) \cdot M_0 \cdot \exp(-\beta \cdot A_0) - 1}} - 1 \quad (20)$$

Owing to the non-linearity of dynamic constants of materials all response characteristics of dam body, as well as fundamental period T_1 , vary with the change of the amplitude of ground acceleration though its predominant period is kept constant. So that, as we have seen in Table 2, k_{em} changes with A_0 under constant value of T . However, the values of the magnification factors at near the crest (A_c/A_0) are so close to each other in the cases of the

periods of ground motions larger than 0.375 (s) as seen in Fig.11 that we can use the same equation for the relationships between M and A_0 in above cases. Thus we assume that the change in k_{em} with A_0 under constant value of T arises only from the variation of the fundamental period due to material non-linearity.

Based on above assumption, the response characteristics of the sliding masses of which potential sliding circles are shallow and located near the crest, that is, those of sliding circles No.2 and No.3 have been examined. Each value of T_1 corresponding to A_0 at the column of sliding circles No.2 and No.3 in Table 2 has been calculated according to Eq. (16) and Eq. (20). Plotting $k_{em} g/A_0$ against T/T_1 Fig.12 has been obtained. The regression curve has been derived as follows

$$\frac{k_{em} \cdot g}{A_0} = \frac{1}{2.72(1 - T/T_1)^4 + 0.446} \quad (21)$$

In above calculation of T_1 the values of h_1 and h_2 have been adopted to be 0.23 and 0.05 respectively which have been applied to the numerical experiments in this paper. The values of M_0 and β are 4.59 and 2×10^{-3} respectively as shown in Fig.11.

The average value of dynamic shearing modulus for micro-strain amplitude G_0 all over the cross section of the analyzed rockfill dam has been about 5870 (kgf/cm², 575260 kPa) and the average density has been 2.0 (gr/cm³, Mg/m³), so that the average velocity of shear wave over the cross section is about 536 (m/s). The height

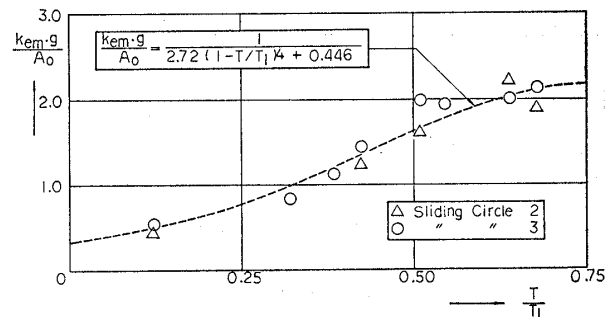


Fig. 12. Relationship between $\frac{k_{em} \cdot g}{A_0}$ and $\frac{T}{T_1}$

of this rockfill dam section is 153 (m), but the depth of cut off is about 10 (m). Therefore the height of shear wedge should be regarded as about 143 (m). Then the fundamental period for micro-strain amplitude ($T_{1,0}$) has been estimated to be 0.7 (s).

Equivalent Sinusoidal Ground Motion for Earthquake Motion

The accelerograms of earthquake motions are generally irregular time histories in both periods and amplitudes and the main factors specifying them are maximum acceleration, predominant period and duration. The synthetic effect of these factors on a structure can be shown by response spectra.

Inputting 11 different accelerograms to the bases of different sorts of grounds at 31 sites in Japan of which layer structures are known, total 341 accelerograms at these surfaces have been calculated with the multiple reflection theory. These 11 accelerograms are the popular ones which are usually applied to the seismic designs for various sorts of structures, that is, Ōfunato 1978 ES, the same NE, Kaihoku-Bridge 1978 TR, and the same LG in the 1978 Miyagiken-Oki Earthquake, Taft 1952 EW, the same NS, Olympia 1949 EW, the same NS, El Centro 1940 EW, the same NS and Golden-gate 1957 EW. Above 31 grounds have various sorts of layer structures so that the predominant periods of the accelerograms calculated with the multiple reflection theory at the surfaces are distributed in the range as wide as possible. Adding 208 accelerograms observed by the Ports and Harbours Research Institute, the Public Works Research Institute, etc. to above ones, total 549 accelerograms have been prepared.

Acceleration response spectra of above 549 accelerograms have been calculated with the damping constant of 0.05, and peak value (S_A) and its predominant period (T_p) for each of calculated spectra have been obtained. The ratio of S_A to the maximum value of corresponding accelerogram (A_{0s}) and T_p have been plotted taking S_A/A_{0s} in logarithmic

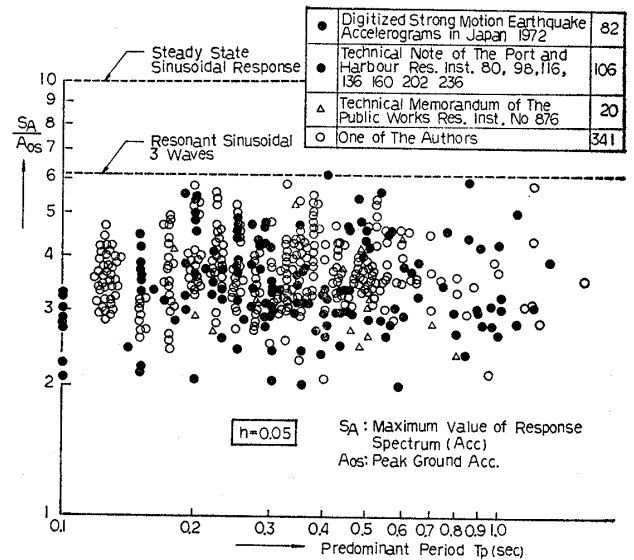


Fig. 13. Response spectra of sinusoidal motion and observed accelerograms

mic scale as the ordinate and T_p also in logarithmic scale as the abscissa, then Fig. 13 has been obtained. It will be seen that the predominant periods of above accelerograms are distributed in the range from about 0.1 (s) to 2.0 (s). So that, it may be said that above range is sufficiently wide to be considered to contain general characteristics of the predominant periods of earthquake motions for dams.

From Fig. 13 it can be concluded that the maximum response accelerations of observed accelerograms are at most about 50 to 60% of those of steady state sinusoidal motions.

Inversely, the amplitude of steady state sinusoidal ground acceleration which gives the same value as the upper bound of response spectra of above 549 accelerograms is only to be 50 to 60% of the peak value of corresponding accelerogram. Besides, it will be observed in each accelerogram of which maximum value of response spectrum is plotted near around the upper bound that the number of waves of which peak values exceed 50 to 60% of the peak acceleration is 7 to 8 and more.

On the other hand, the maximum response spectrum of sinusoidal motion with resonant frequency is $1/2 h (1 - e^{-2\pi h N})$, where N is the number of waves, and its value becomes

to be more than 90% of steady state one for N of 8 and more. That is, such sinusoidal motions can be approximately regarded as steady state ones. All waves being included in above number of waves are not necessarily to have same frequency, so that above sinusoidal motions tend to produce excessive values of response spectra, that is, the ones in conservative side.

As for the accelerograms of which maximum values of response spectra are small [away from the upper bound, the amplitudes of steady state sinusoidal motions producing the same response spectra must be considerably lower than above one, and so adopting the same level as above one for the amplitudes the corresponding number of waves become to be smaller. These accelerograms may be said to have only a little ability to generate the sliding in the dams.

Thus, we propose in this paper that 0.5 to 0.6 of the maximum acceleration of design earthquake motion and the number of waves (N) of which peak values exceed above value should be adopted as the amplitude and number of equivalent sinusoidal ground acceleration. And it will be natural to adopt the predominant period of original motion for the period of the equivalent sinusoidal one.

Allowable Sinusoidal Ground Acceleration Corresponding to Given Critical Deformation at Near Crest

Representing amplitude of acceleration, predominant period and number of repetition of the equivalent sinusoidal ground motion obtained above as A_0 , T (for T_p) and N respectively and substituting Eq. (21) into Eq. (11) we have obtained following expression.

$$A_0 = 335 \cdot g \left[\left(1 - \frac{T}{T_1} \right)^4 + 0.164 \right] N^{-3/2} \cdot \left(\frac{D_f}{H} \right)^{3/5} \quad (22)$$

If the allowable sliding displacement at near crest D_f is given we can estimate the critical amplitude of equivalent sinusoidal ground acceleration from Eq. (22) with each

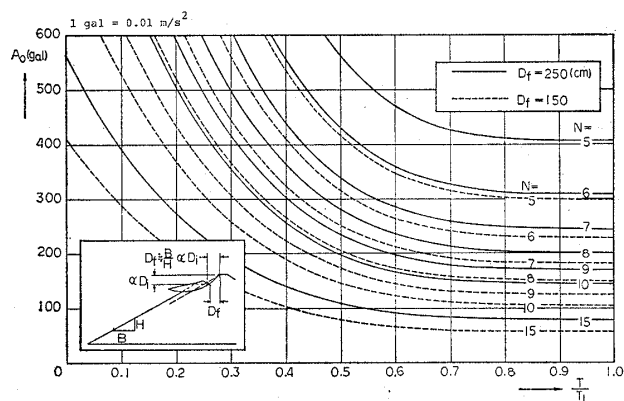


Fig. 14. Allowable equivalent sinusoidal ground acceleration corresponding to given critical deformation near crest

value of parameters N and T/T_1 . Examples thus calculated for the cases of $D_f=250$ (cm) and $D_f=150$ (cm) are shown in Fig. 14. In the figure letting D_i be a margin height of a dam and letting $100 \cdot \alpha\%$ of D_i be the allowable settlement due to sliding, then the allowable horizontal displacement D_f may be approximately estimated as $\alpha \cdot D_i$ (B/H) where $H : B$ represents the slope of the surface of a rockfill dam. Assuming the margin height to be 2 meter, then $D_f=250$ (cm) is to be corresponding to the allowable settlement due to sliding of about 48% of the margin height.

The validity of Eq. (22) has been examined for the cases E(300) and E(200) in Table 1. In these cases the predominant period of El Centro 1940 NS (T) and the number of waves of which peak accelerations exceed 0.6 of the maximum acceleration (A_{0s}) have been estimated to be about 0.5 (s) and 8 times respectively, and the values of T/T_1 have been estimated from Eqs. (16) and (20) as to be 0.524 for the case E(300) and 0.560 for the case E(200) respectively by putting A_0 equal to $0.6 A_{0s}$. The values of D_f of the mass on potential sliding circle No.3 where the maximum displacement has been generated among all potential circles have been calculated to be 125 (cm) for the case E(300) and 87 (cm) for the case E(200) as shown in Table 3. Substituting these values into D_f in Eq. (22) and putting N equal to 8, then the value of A_0 has been calculated

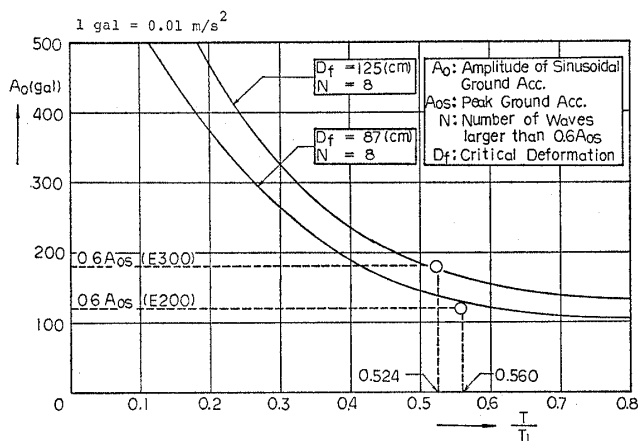


Fig. 15. Equivalent sinusoidal ground acceleration generating same deformation as one due to earthquake motion

for each value of T/T_1 . Above results have been shown in Fig.15 by solid lines. The values of $0.6 A_{0s}$ for above two cases have been superimposed in Fig.15. It may be seen that the agreement is well.

CONCLUSIONS

Summarizing the above discussions the following conclusions have been obtained.

(1) The relationship between the factor of safety (F_s) and the equivalent instantaneous seismic coefficient (k_e) at every moment obtained from dynamic response analysis of rockfill dams coincides well with the one between the factor of safety and seismic coefficient obtained from conventional pseudostatic method, that is, the factor of safety with respect to sliding is to be nearly equal if only the load or the seismic coefficient applied to the sliding mass is same, though the method of analysis is different.

(2) A simple formula concerning with the relationship between the horizontal sliding permanent displacement per a period due to sinusoidal ground motion (D_R), duration of sliding (t_d) and the amplitude of the equivalent instantaneous seismic coefficient (k_{em}) of arbitrary sliding mass has been obtained and written in the following form.

$$D_R = \frac{1}{2} (k_{em} \cdot g) \cdot t_d^2$$

Above formula is independent of the scale and location of sliding surface, the period of ground motion and the amplitude of ground acceleration.

(3) A simple formula concerning the relationship between the sliding permanent displacement due to ground earthquake motion (D_f), the number of equivalent sinusoidal ground waves (N) and the amplitude of the equivalent instantaneous seismic coefficient on arbitrary sliding circle (k_{em}) due to the equivalent sinusoidal ground motion has been obtained and written in the following form.

$$k_{em} \cdot g = 123 \cdot g \cdot \left(\frac{D_f}{H} \right)^{3/5} \cdot N^{-3/2}$$

(4) With acceleration spectra calculated on 549 accelerograms with the damping constant of 0.05 it has been clarified that the maximum response acceleration of observed accelerograms are at most 50 to 60% of those of steady state sinusoidal motion and it has been proposed that 0.5 to 0.6 of the maximum acceleration of design earthquake motion should be adopted as the amplitude of equivalent sinusoidal ground acceleration and that the number of the waves of which peak acceleration exceed above value with the predominant period should be adopted as the duration.

(5) A simple formula concerning with allowable sinusoidal ground acceleration corresponding to given critical deformation at near crest has been obtained in the following form.

$$A_0 = 335 \cdot g \left[\left(1 - \frac{T}{T_1} \right)^4 + 0.164 \right] N^{-3/2} \cdot \left(\frac{D_f}{H} \right)^{3/5}$$

A diagram concerning to above relationship has been proposed.

NOTATION

- A_0, A_c = amplitudes of steady state sinusoidal accelerations at the base and the crest of dam respectively
- A_{0s} = the maximum acceleration of ground earthquake motion
- D_f = sliding permanent displacement due to earthquake motion

- D_R = sliding permanent displacement per a period due to sinusoidal ground motion
- F_S = factor of safety
- G, G_0 = dynamic shearing moduli of arbitrary strain amplitude and micro-strain amplitude respectively
- g = acceleration of gravity
- H = height of dam
- h = damping constant of dam materials
- h_1, h_2 = maximum value of damping constant measured by dynamic tri-axial compression test and radiating dissipation damping constant respectively
- k_e = equivalent instantaneous seismic coefficient
- k_{em} = amplitude of k_e due to sinusoidal ground motion
- k_H = horizontal seismic coefficient
- k_R = yielding seismic coefficient
- l_i = length of sliding line cut out by the " i "-th element
- $M = A_c/A_0 = M_0 \cdot \exp(-\beta \cdot A_0)$
- m = mass on a potential sliding surface
- N = number of sinusoidal ground waves equivalent to earthquake motion
- S_A = peak value of acceleration response spectra
- T or T_p = predominant period of earthquake motion
- T_1 = fundamental period of fill dam
- $T_{1,0}$ = fundamental period of fill dam for micro-strain amplitude
- t_d = duration of sliding per a period due to sinusoidal ground motion
- t_f = duration of sliding due to earthquake ground motion
- $\alpha(x, y)$ = response acceleration on any point in sliding mass
- β = coefficient in the exponent of M
- β^* = angle between the radius of the sliding circle passing through the center of gravity of sliding mass and the vertical
- γ = amplitude of shearing strain
- γ_r = reference strain
- $\rho(x, y)$ = density on any point in sliding mass
- τ = deviation of the fundamental period due to non-linear material properties
- τ_i = acting shearing stress along sliding surface
- τ_{Ri} = resisting shearing stress along sliding surface
- ϕ = angle of internal friction

REFERENCES

- 1) Baba, K. and Watanabe, H. (1979) : "On a consideration for an earthquake-resistant design method for rockfill dams," Trans. of the 13th Congress on Large Dams, New Delhi, Vol. II, pp. 1049-1074.
- 2) Matsumura, M. (1934) : "Deformation of earth dams during earthquakes," Public Works Research Institute Report No. 28.
- 3) Newmark, N. M. (1965) : "Effects of earthquakes on dams and embankments," Fifth Rankine Lecture, Géotechnique 15, No. 2, pp. 139-160.
- 4) Nakamura, K. et al. (1982) : "Dynamic deformation analysis of an embankment," Proc. of the 17th Japan National Conference on Soil Mechanics and Foundation Engineering, pp. 1889-1892.
- 5) Sasaki, Y. et al. (1982) : "One method of calculating permanent deformation of embankment due to earthquake," Proc. of the 17th Japan National Conference on Soil Mechanics and Foundation Engineering, pp. 1893-1896.
- 6) Seed, H. B., Lee, K. L., Idriss, I. M. and Makdisi, F. (1973) : "Analysis of the slides in the San Fernando Dams during the earthquake of February 9, 1971," Report No. EERC 73-2, Earthquake Engineering Research Center, University of California, Berkeley.
- 7) Seed, H. B. (1979) : "Consideration in the earthquake-resistant design of earth and rockfill dams," the Rankine Lecture 1979, Géotechnique 29, No. 3, pp. 215-263.
- 8) Watanabe, H. (1972) : "Methods of numerical analysis in seismic stability analysis of fill dams," Technical Report No. 72007, Civil Engineering Laboratory, CRIEPI.
- 9) Watanabe, H. (1977) : "A consideration on the seismic coefficients of rock and earth fill dams through observed accelerograms and model tests," Proc. of 6th World Conference on Earthquake Engineering, New Delhi, India.
- 10) Watanabe, H. and Baba, K. (1981) : "A consideration on the method of evaluation for sliding stability of fill dams against earthquake motion on the basis of dynamic response analysis," JANCOLD, Jour. of the Japanese National Committee on Large Dams, No. 97.